Agyakwa, Pearl and Yang, Li and Corfield, Martin and Johnson, Christopher Mark (2014) A non-destructive study of crack development during thermal cycling of Al wire bonds using x-ray computed tomography. In: 8th International Conference on Integrated Power Electronics Systems, 25-27 February 2014, Nuremberg, Germany.

A non-destructive study of crack development during thermal cycling of Al wire bonds using x-ray computed tomography

Pearl A Agyakwa*, Li Yang, Martin R Corfield & C Mark Johnson
Department of Electrical & Electronic Engineering, The University of Nottingham, University Park, Nottingham, NG7 2RD, UK.
*Corresponding author: Tel.: +44(0)1158466890 Email: pearl.agyakwa@nottingham.ac.uk

Summary / Abstract

This paper concerns the non-destructive visualisation of the evolution of damage within ultrasonically bonded aluminium wires using three dimensional x-ray computed tomography. We demonstrate the potential to observe the progressive accumulation of damage within the same wires during passive thermal cycling between -55°C and 190°C. Tomography datasets were obtained prior to and after cycling. Cracks could be seen emerging from the extreme ends of the bonds when imaged after 105 cycles. Subsequent cycling lead to the advancement of these cracks toward the centres of the bonds. In addition, damage developed within the interior of the bonds; these also grew with increase in number of cycles, and merged with existing cracks. Virtual cross-sections have been analysed to quantify the rate of damage build up.

1 Introduction

The cracking and lifting off of wire bond interconnects is perhaps the most prevalent and life-limiting wear out mechanism in power modules [1, 2]. Thus, our ability to realise effective reliability predictions for power modules is hinged on our understanding of wire bond wear-out mechanisms. Congruently, the integrity of such lifetime prediction models depends strongly on the quality of the experimental data from which they are derived or with which they are validated. Typically, traditional wear-out data may consist of counts of lift-off events as a function of time, or “after the event” analyses such as SEM fractography of the lifted off wires. Other data may be derived from “macrostructure of damage” analyses obtained from “interrupted tests”, whereby a number of samples would be sacrificed for shear tests or metallurgical cross-sectioning at certain pre-determined points during a stress experiment.

The justification for the use of shear force is that it decreases to reflect the reduction in bonded area which accompanies crack propagation during cycling. This, however, may not be strictly accurate, as a reduction in shear (and pull) strength may also be attributable to a change in a material’s yield strength. This is particularly relevant to extended thermal cycling regimes, in which the characteristically high temperatures may lead to significant microstructural restoration [3]; thus a wire bond interconnect which remains adequately intact may be wrongly characterised as lifting off.

Metallurgical cross-sections are a helpful approach to obtaining crack growth rates [4, 5]. However, as only one of an infinite number of potential planes is usually examined, such data may be at risk of misinterpretation and of inconsistencies and inaccuracies which exaggerate or underestimate the real spread of the data.

Wire bond lifetime evaluation data may also involve forward voltage measurements as a function of number of cycles. This approach has been shown to lack sufficient sensitivity of the critical wear-out period, as it only begins to detect degradation once several lift-offs have already occurred. Shear tests and metallurgical cross-sections may be an improvement in terms of sensitivity; however, they also have some drawbacks as stated previously, and crucially, their destructive nature does not allow the same specimen to be monitored and evaluated over an entire test period.

In recent years, the non-destructive observation of the internal structure of engineering materials and structures has become greatly facilitated by x-ray computed tomography [6, 7, 8, 9]. Because a specific specimen can be evaluated over its lifetime, a true picture of the evolution of damage during operation can be obtained, and cracks and defects can be observed three-dimensionally. To the authors’ best knowledge, such data is not reported in the literature for wire bond wear-out. A major advantage of 3D x-ray computed tomography is the possibility to scrutinise the bond interface of a wire bond and track the evolution of damage from the outset. In addition, it offers the possibility of obtaining multiple virtual cross-sections. Furthermore, the opportunity to observe damage in three-dimensional space may provide a unique perspective on crack development. The mechanism of wire bond lift-off due to thermal cycling fatigue is well documented [1, 2, 10]. However, in recent years, a more detailed and complex picture of fatigue has been emerging. For instance, it has been suggested that fatigue crack propagation is rather heterogeneous in nature, and that propagation rates within the interior and at the surface may differ greatly under different fatigue stress conditions [7, 9, 11]. In this respect, additional insight attainable from x-ray computed tomography is both unique and invaluable, particularly in relation to the development of constitutive models.

The use of 3D x-ray tomography to observe cracks in bond wires is however still nontrivial. As a rule, tomography imaging of a power module package is not easily achieved due to the rather large x-ray absorption characteristics of its high Z element constituents, such as copper, tin and silver. Fortunately, as only the aluminium wire bonds are of interest in this work, this limitation can be avoided by adopting a mounting strategy which allows the best possible transmission and ample counts to be achieved at the detector. Another challenge usually encountered is the resolution of fine features, such as cracks and openings (1-3µm) in relatively large specimens (see Figure 1), as large specimens usually limit the achievement of optimal detector-sample and source-sample distances. In this paper, work is performed on a Versa-XRM 500 machine, supplied by Carl Zeiss X-ray Microscopy. This model is unlike most other microCT platforms in that it utilises a turret of objectives, thus facilitating two-stage magnification (geometric and optical), and also has large source and detector working distances.

In this paper, we demonstrate the potential of x-ray tomography to observe the progressive accumulation of damage within ***the same*** ultrasonically bonded aluminium wires during passive thermal cycling between -55°C and 190°C.

2 Experimental

2.1 Wire bonding and thermal cycling

A standard substrate tile from a half-bridge IGBT module supplied by Dynex Semiconductor Ltd was investigated. This consists of 375µm thick aluminium wires ultrasonically bonded onto Al-metallised silicon diodes and IGBTs (see Figure 1). In this work, we report on detailed investigation of four individual wires bonded onto a diode, as indicated in Figure 1. The bonds were subjected to passive thermal cycling from -55 to 190°C in an environmental chamber.

2.2 X-ray tomography and image analysis

The accumulation of damage within the same ultrasonically bonded aluminium wires during passive thermal cycling was studied. The wires were imaged prior to thermal cycling (in the "as-bonded" condition) in order to provide a basis for comparison. The same wires were subsequently imaged after 105, 215, 517 and 867 cycles. A source voltage of 80kV was used and a 4X objective detector was selected. Specimen-to-source and specimen-to-detector distances were typically 28 mm and 90 mm respectively. An appropriate filter was applied to minimise beam hardening effects. A 2x2 camera binning mode was used to capture the images at exposure times per projection ranging between 9 and 15 seconds; these parameters allowed a pixel size of about 1.6 µm to be achieved, which was considered adequate for the resolution of cracks and openings. For each specimen, a total of up to 2400 projections were acquired over a rotation span of 180°.

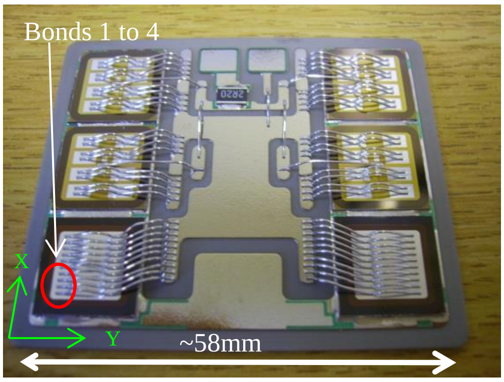

Figure 1 Substrate tile investigated. Bonds analysed in detail are denoted by the red circle.

3 Results and discussion

In Figure 2, a volume rendered image is presented giving an overview of a typical scanned volume. The imprint of the wedge tool can be clearly seen on the exterior of the wires.

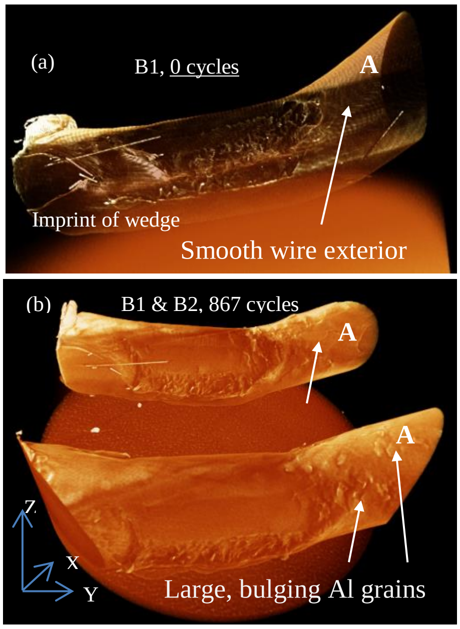

Figure 2 Volume rendered images of Bonds 1 &2 provide an overview of the region of interest.

At zero cycles, the wire exterior (region a marked '**A**' in Figure 2a), appears relatively smooth. This evidently changes after several thermal cycles (Figure 2b), when 'bulging' of large grains and grain boundaries becomes apparent in the same region. This is a well-known nucleation mechanism during the dynamic recrystallisation of single phase polycrystalline materials [12] and is thought to result from strain-induced grain or subgrain boundary migration [13]. In our case, the basis of this may be the non-isothermal state and/or localised strains from the mismatch of coefficient of thermal expansion resulting in high amounts of stored energy at grain boundaries. This would be in agreement with previous observations of recrystallisation, recovery and grain growth during the thermal cycling of aluminium wire bonds [3, 14, 15].

Virtual cross-sections are presented from planes parallel to the interfaces of the wire bonds prior to and after cycling. These give a plan view of the structure of damage as it appears during cycling. Figure 3 shows Bond 1 from the as-bonded condition right through to 867 cycles. It exhibits the characteristic shell-nut shape associated with bond footprints. Prior to cycling (Figure 3a), a small crack (annotated by a red arrow) is evident on the right hand side, which also happens to be the heel side. It is usual to find cracks at the heel of a bond prior to thermal cycling. These usually come about due to wire flexure during bonding, and tend to act as the initiation site for subsequent propagation. Besides this pre-crack, the interface appears free of damage and there are no visible cracks or voids at zero cycles.

However, damage can be seen beginning to appear at the extreme corners of bond interface after 105 cycles (see Figure 3b). These cracks appear to advance towards the interior of the bond with increasing number of cycles. This is consistent with other microstructural observations [5, 8], and seems slightly more extensive on the right hand side, where the pre-crack was located.

Additionally, it is interesting to observe a small number of micro-defects, from a few microns upwards in size, which appear within the interior of the bond foot after 105 cycles; these seem to grow, coalesce and/or increase in number during further thermal cycling (a number of these are annotated by *a*, *b*, *c* and *d* in Figures 3b, c, d & e). A similar observation was made by Tsuritani *et al.* in relation to solder ball joints [8, 16]. Although the formation and coalescence of voids is a known mechanism of high temperature failure in ball bonds, for example, its relevance in Al-Al bonds in power applications is not yet clear. If these are indeed voids, then the plausibility of the concurrence of diffusion or creep related voiding with fatigue cracking at Al-Al bond interfaces (perhaps only relevant under extreme temperature conditions) must be examined. It is also possible that these micro-defects originate from sub-resolution regions of partial bonding, although these were not discernible in the tomography datasets acquired *ab initio*.

A schematic representation of the evolution of damage is given in Figure 4. This clearly shows the progressive reduction in bonded area with increasing number of cycles.

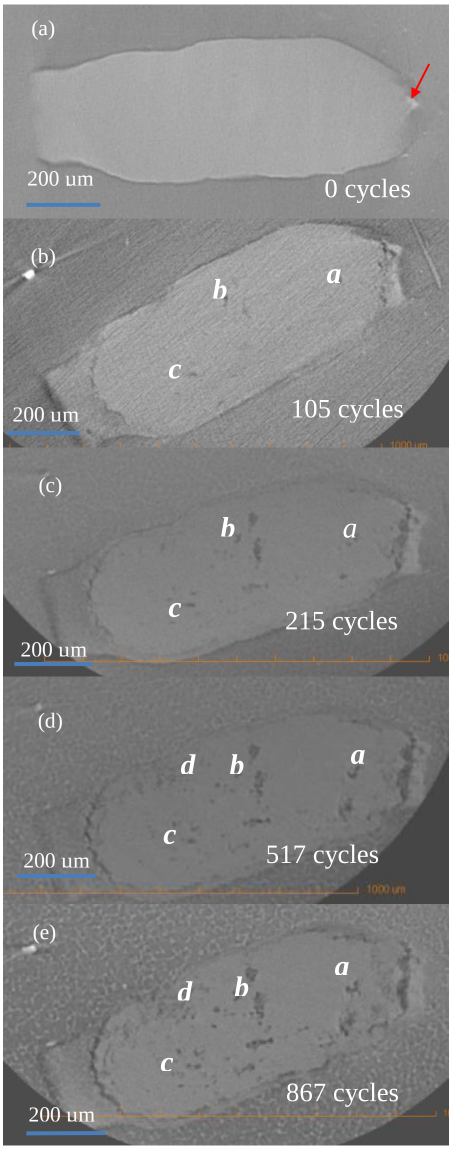

Figure 3 Virtual cross-sections in the X-Y plane of the interface of Bond 1 (B1)

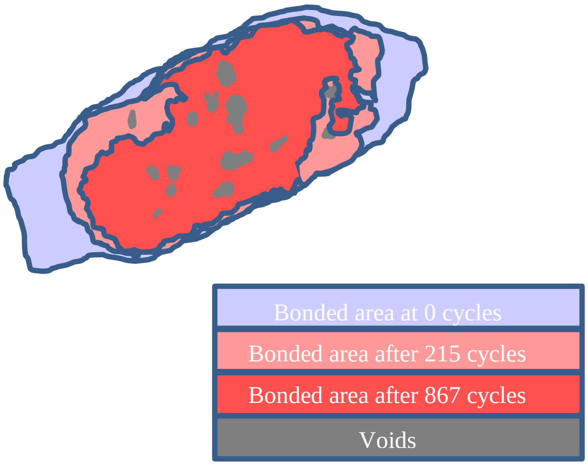

Figure 4 Schematic 2D representation of damage evolution in X-Y plane with number of cycles

To further illustrate the damage observed in the X-Y plane (plan views), virtual cross-sections in the more familiar Y-Z plane have been made at mid-thickness of Bond 2 at zero cycles (Figures 5a and 5b) and at 517 cycles (see Figure 5c and d).

Additional virtual cross-sections are presented in Figure 6 showing how the internal damage observed after 867 cycles appears in cross-sections made along the XZ plane (indicated by the red lines).

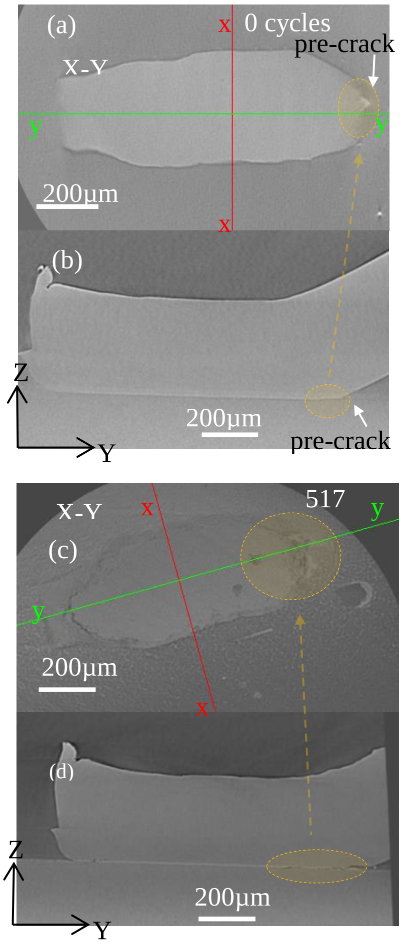

Figure 5 Virtual cross-sections in the X-Y and Y-Z planes of Bond 2.

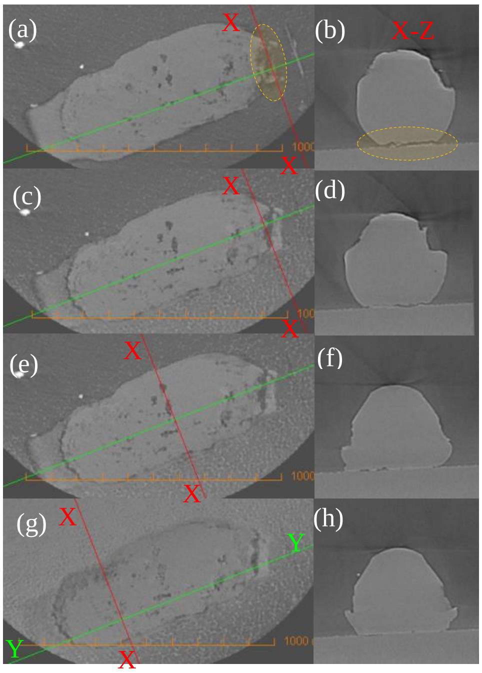

Figure 6 Virtual cross-sections illustrating the damage within Bond 1 in the X-Y and X-Z planes.

An uncomplicated approach to quantifying the evolution of damage has been employed which involves simply estimating the surface area of damage visible within the two-dimensional greyscale TIFF images obtained parallel to the bond interface. This was performed for the four wire bonds using the polygon selection tool within *ImageJ* software and the results are plotted in Figure 7. The evolution of damage is expressed as fraction of area bonded as a function of the number of cycles. The fraction of area bonded f_a is close to 1 in the as-bonded condition and tends to zero as thermal cycling progresses. For comparison, crack propagation data from metallurgical cross-sections data presented by Yamada *et al.* [18] for two similar thermal cycling regimes have been plotted on the same axes. Degradation rates are similar for both sets of data; thus it can be concluded that the quantitative data obtained from virtual cross-sections give reasonable and representative results.

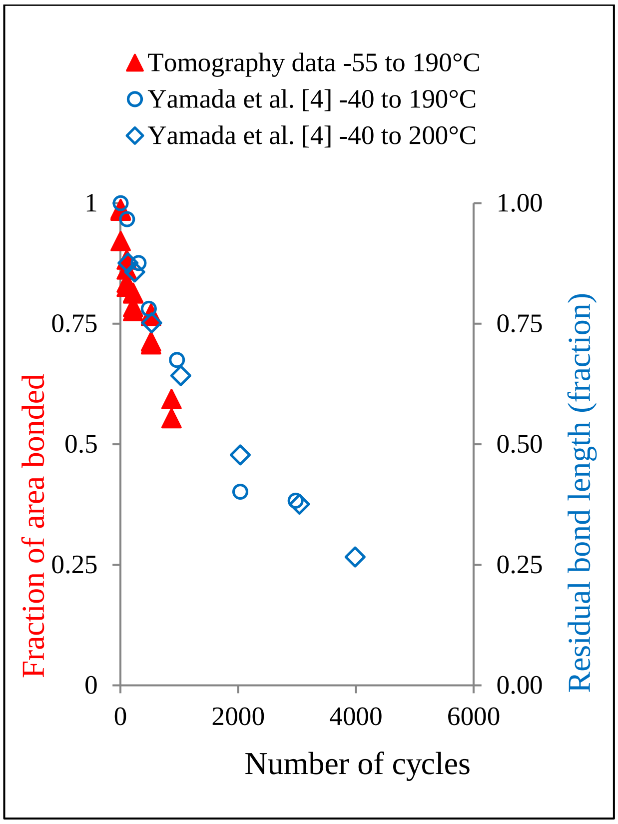

Figure 7 Fraction of area bonded versus number of cycles for Bonds 1 to 4, compared to Yamada *et al.* [18].

4 Summary and conclusions

In this paper, 3D x-ray microscopy has been utilised to visualise cracks and voids as they evolve at the interface of the same ultrasonically bonded aluminium wires subjected to passive thermal cycling from -55 to 190C. Cracks were observed to emanate from the extreme edges of the bonds and advance towards the centre. In addition, micro-defects, which may be voids or micro-cracks, have been observed within the interior, which apparently grow with increase in number of cycles. The crack propagation rate measured by virtual cross-sections compares favourably with what has been reported for similar thermal cycling ranges. In future work, this data will be compared to shear force reduction data for similar thermal cycling regimes. The wire bonds in this study will be imaged using x-ray microscopy until lift-off. Additionally, further work is planned to determine whether there are any differences in the way damage evolves at the interface under different thermal cycling profiles.

5 5 Acknowledgments

The authors gratefully acknowledge the support of the Innovative Electronics Manufacturing Research Centre (IeMRC) funded by the UK Engineering and Physical Sciences Research Council (EPSRC) through research grant EP/H03014X/1. The authors also wish to thank Dynex Semiconductors Ltd. for providing the bonded substrate tiles.

6 References

[1] M. Ciappa, Microelectron. Reliab. 42 (2002) 653–667

[2] I. Lum, M. Mayer, & J. Zhou, J. Electron. Mater. 35 (2006) 433–442

[3] P A Agyakwa, W S Loh, M R Corfield, JF Li, E Liotti, S C Hogg, C M Johnson, , IEEE TDMR 10:2 (2010) 254-262

[4 Y. Yamada, Y. Takaku, Y. Yagi, I. Nakagawa, T. Atsumi et al., Microelectron. Reliab. 47 (2007) 2147–2151

[5] J Onuki, M Koizumi M Suwa, IEEE Trans. Adv. Pack. 23 (2000) 108-112

[6] P.J. Withers & M. Preuss, Annual Review of Materials Research 42 (2012) 81-103

[7] H. Zhang, H. Toda, P.C. Qu, Y. Sakaguchi, M. Kobayashi, K. Uesugi , Y. Suzuki, Acta Mat. 57 (2009) 3287–3300

[8] H. Tsuritani, T. Sayama, Y. Okamoto, T. Takayanagi, K. Uesugi, T. Mori, J. Electron. Packaging 133:2 (2011) 021007

[9] P.J. Withers, Nature Mater. 12:1 (2013) 7-9

[10] S. Ramminger, S P. Turkes, G. Wachutka, Microelectron. Reliab. 38 (1998) 1301-1305

[11] J.Y. Buffiere, E. Maire, J. Adrien, J.P. Masse, E. Boller, Exp. Mech. 50:3 (2010) 289-305

[12] F.J. Humphreys, “Recrystallization and Related Annealing Phenomena” Elsevier Science Ltd, Oxford, UK, 1996.

[13] D.K. Sun, C.P. Chang, P.W. Kao, Metall. Mater. Trans A. 41(2010) 1864-1870

[14] P.A. Agyakwa, M.R. Corfield, L. Yang, J.F. Li, V.M.F. Marques, C.M. Johnson, Microelectron. Reliab. 51:2 (2011) 406-415.

[15] PA Agyakwa, VMF Marques, MR Corfield, JF Li, L Yang, CM Johnson, J. Electron. Mater.42:3 (2013) 537-544.

[16] H. Tsuritani, T. Sayama, K. Uesugi, T. Takayanagi, T. ; Mori, T, J. Electron. Packaging 129:4 (2007) 434-439